

PREDICTION OF FIBRE ORIENTATION AND STIFFNESS DISTRIBUTIONS IN PAPER – AN ENGINEERING APPROACH

Torbjörn Wahlström

Stora Enso AB, Publication Paper R&D, Box 9090, 650 09 Karlstad, Sweden,
torbjorn.wahlstrom@storaenso.com

ABSTRACT

The orientation of the fibres in a paper directly influences many of its properties. The focus of this work was to predict the fibre orientation distribution and tensile stiffness distribution of a paper. The predictions were based on a proposed link between the two distributions and physical parameters measurable on the paper, no fitting parameters.

The fibre orientation distribution in paper was approximated by a probability density function. Both curve fitting type of distribution functions earlier used in paper physics and physical based functions derived from Fluid mechanics, Orthotropic analysis and a simple Stress/strain analysis were evaluated. The physical based functions used one measurable physical parameter, the fibre orientation anisotropy. The tensile stiffness distribution was predicted with a distribution function from the literature and functions derived from the Fluid mechanics and Orthotropic analysis approach. The predictions needed two measurable physical parameters, the MD and CD tensile stiffness.

Predictions of fibre orientation distribution and tensile stiffness distribution for restrained dried papers were compared with experimental data from restrained dried oriented handsheets with varying fibre orientation anisotropy. General approaches valid for

all papers were compared with experimental data from pilot made papers with different drying restraint history. Both the predicted results for fibre orientation distribution and tensile stiffness distribution showed good agreement with experimental data.

INTRODUCTION

In papermaking wood fibres are mixed with water to a furnish with a fibre concentration of around 0.5%. In the head box of the paper machine the furnish is accelerated close to the manufacturing speed of the papermachine. When entering the forming section the furnish, now referred to as mix, is further accelerated or decelerated by the forming fabric to machine speed. Before entering the headbox the orientation of the fibres can be treated as randomly distributed. The characteristics of the flow thereafter will affect the fibres and more or less align them in the direction of the flow (The manufacturing direction, MD).

There are two basic mechanisms that orient fibres in a flowing suspension, shear fields and accelerating flow. The most typical shear field is a surface moving in parallel to a static surface. In contact with the surfaces the fluid will have the same speed as the surfaces giving a principal velocity field as shown in Figure 1. Considering that the velocity at the top of the fibre is higher than the velocity at its other end, the fibre will rotate and align with the flow. An accelerating flow, as shown in Figure 2, will also align the fibres with the direction of the flow since the flow velocity also in this situation differ at

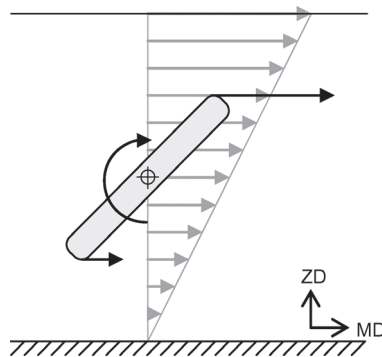


Figure 1. A fibre in a shear flow (schematic for mix to wire interaction) seen from a side view. Rotation in the MD/ZD plane.

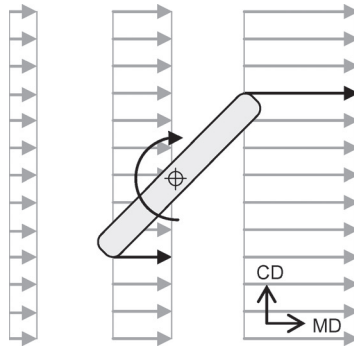


Figure 2. A fibre in an accelerating flow (schematic for headbox contraction) seen from above. Rotation in the MD/CD plane.

the different ends of the fibre. In the papermaking process the flow can schematically be treated as accelerating in the headbox nozzle contraction and shearing when the mix meets the forming fabric.

The alignment of the fibres means that if the number of fibres in different directions are observed the amount of fibres in MD increases and consequently the amount of fibres in the perpendicular direction CD (Cross Direction) decreases. The ratio of the amount of fibres in MD and CD is normally referred to as the fibre orientation anisotropy. Likewise the ratio of a paper property in MD and CD is usually referred to as the anisotropy of that property, for example tensile stiffness anisotropy. Considering only the fibre orientation distribution (Neglecting drying effects etc) a paper with random fibre orientation distribution has the same paper properties in all directions (isotropic) and the in-plane anisotropy is one. A speed increase of the furnish as referred to above will increase the fibre anisotropy, whereas turbulence in the headbox is known to reduce the fibre anisotropy. A differential speed between the mix and wire will also increase the anisotropy. The number of fibres oriented in a certain direction will have a direct influence on the paper properties in this direction. For example increased fibre anisotropy gives increased strength anisotropy.

Several research groups are active in understanding of the detailed mechanisms creating fibre orientation (Hyensjö 2008, Hämäläinen and Hämäläinen 2007, Jäsberg 2007, Krochak 2008, Lindström and Ueseka 2008, Parsheh *et al.* 2005). Among other things the shape and rigidity of the fibres and the characteristics of the flow, the headbox geometry and the concentration of fibres has to be considered. To predict a certain fibre orientation distribution based on the papermaking process has many applications, such

as describing the paper, process understanding and machine component design. The intention with this work is however only to find a useful description of paper, its properties and structure, not the mechanisms active in creating the same.

In this work the fibre orientation distribution will be predicted with approximations based on the fibre orientation anisotropy as measurable physical parameter. Also the tensile stiffness distribution will be predicted based on tensile stiffness in MD and CD as measurable physical parameters. Both earlier used distribution functions and three new physical based functions derived from Fluid mechanics, Orthotropic analysis and a simple Stress/strain analysis are evaluated. Predictions of fibre orientation distribution and tensile stiffness distribution for restrained dried papers will be compared with experimental data from handsheets with varying fibre orientation anisotropy. Predictions of tensile stiffness distribution will also be compared with experimental data from handsheets with different drying restraint history. It will also be shown that the proposed distributions exhibit a well known behaviour for paper. Namely that the geometric mean of MD and CD tensile stiffness at restrained drying is constant (invariant) and equal to the isotropic value with varying fibre orientation anisotropy.

MATERIALS AND METHODS

Papermaking

For the fibre orientation distribution measurements a CTMP pulp (Freeness 411 CSF) from a board mill was used. Handsheets were made with three fibre orientation anisotropies, A_F , Low, Medium and High. The speed of the Formette drum was 1100 rpm and the nozzle pressure 2.0; 2.5 and 3.0 bars were used for the different fibre anisotropies. The conditioned basis weight was 80 g/m². Pressing was done in a roll press, first pressing at 250 kPa and secondly at 450 kPa. The samples were dried restrained in a STFI plate dryer.

For the stiffness distribution measurements, for different fibre orientation anisotropies, a furnish from the middle ply machine chest of a board mill was used. The furnish (22.5° Schopper Riegler, SR) contained CTMP, low yield sulphate, broke and a small amount highly refined sulphate. Anisotropic handsheets were made in a Formette dynamic sheet former with a conditioned basis weight of 110 g/m² for restrained dried sheets. The speed of the drum was 1100 rpm and a nozzle pressure of either 2.0; 2.5 or 3.0 bars were used to produce three different fibre anisotropies, Low, Medium and High.

For the stiffness distribution measurements for different drying restraints a bleached kraft softwood pulp, beaten to 25 SR in an industry-style refiner,

was used. Paper was made on STFI's pilot paper machine EuroFEX. The anisotropy in Tensile stiffness (MD/CD) for a restrained dried sample of the paper was 2.3 and the basis weight 61 g/m² measured at 23°C and 50% relative humidity. The wet papers were pressed in the Pilot machine to a dry solids content of 42% and dried with different combinations of free and restrained drying in MD and CD in a biaxial dryer (Wahlström *et al.* 2000).

Measurements

Fibre Orientation Distributions were measured by Stora Enso Karlstad Research Centre using an image analysing method. A transparent adhesive tape was applied to both sides of the sample and then the tapes were pulled apart, leaving a layer of fibres on each of the two tapes. A new tape was applied to the delaminated surface and the tapes were pulled apart again etc. The samples in this study were separated into about 25 layers. A reflectance image against black background was produced on each layer using a scanner. The images were subsequently analysed to determine the fibre segment angle distribution of each layer as a measure of fibre orientation. Thereafter a von Mises distribution function was fitted to the experimental data for each layer. The analysis and parameter definitions are described in detail by Rigdahl and Hollmark (1986). The average of the evaluated fibre orientation distributions from each layer was used as the fibre orientation distribution of the sample.

The Tensile stiffness index distributions were measured using an L&W TSO tester (Lindblad 1996). Tensile stiffness index, E , was calculated in eight in-plane directions from the speed, v , of an ultrasonic pulse in each direction using $E = v^2(1 - 0.293^2)$.

Trial program

Fibre orientation distributions. – Fibre orientation distribution was measured on handsheets with three different anisotropies. The experimental results were compared with predictions using distribution functions from the literature and new approximations.

Tensile stiffness distributions for varying fibre orientation anisotropy. – Tensile stiffness index distribution was measured on restrained dried handsheets with three different anisotropies. The experimental results were compared with predictions using proposed approximations.

Tensile stiffness distributions for varying drying restraints. – Tensile stiffness index distribution was measured on pilot made paper dried with different

drying restraints in MD and CD. The experimental results were compared with predictions using proposed approximations.

Invariance of the distribution functions. – It was evaluated if the proposed distribution functions exhibit the well known behaviour of paper that the geometric mean of MD and CD tensile stiffness at restrained drying is constant (invariant) and equal to the isotropic value with varying fibre orientation anisotropy.

DISTRIBUTION FUNCTIONS

Fibre orientation distributions – previous work

General. – Fibres in machine made papers are oriented at different angles, γ , in the plane of the paper. Assume that the fraction of the total number of fibres oriented between γ and $\gamma + d\gamma$ is $d\gamma/\pi$, where γ is an angle to a reference direction and lies between $-\pi/2$ and $\pi/2$. Then Equation 1 describes a distribution function, expressed as a probability density function, where $\Psi(\gamma)$ describes the variation of the fibre orientation in the plane of the paper. Figure 3 shows a typical example of $\Psi(\gamma)$ for an oriented paper plotted in cartesian and polar form. The angle γ is given in degrees in the plot but in the calculations radians are used. In the following sections an overview of previous work is given and three new derivations of $\Psi(\gamma)$ are presented.

$$\int_{-\pi/2}^{\pi/2} \Psi(\gamma) d\gamma = 1 \quad (1)$$

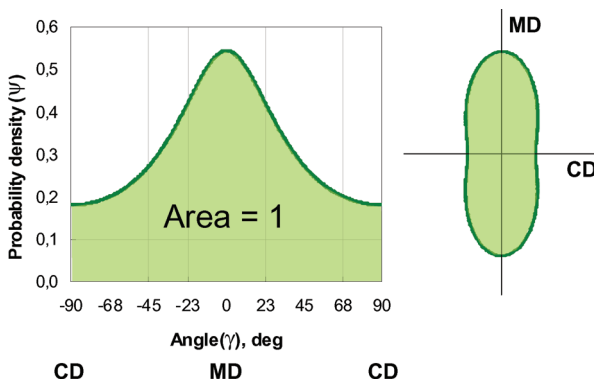


Figure 3. Typical fibre orientation distribution in the plane of an oriented paper expressed as a probability density function.

Isotropic. – Fibres in standard laboratory made handsheets are oriented isotropically (*Iso*) or at random angles in the plane of the paper. Then the probability density function $\Psi(\gamma)$ is constant in the plane of the paper and equal to $1/\pi$ according to Equation 2. Figure 4 shows the fibre orientation distribution for an isotropic paper plotted in cartesian and polar form.

$$\Psi(\gamma)_{iso} = \frac{1}{\pi} \quad (2)$$

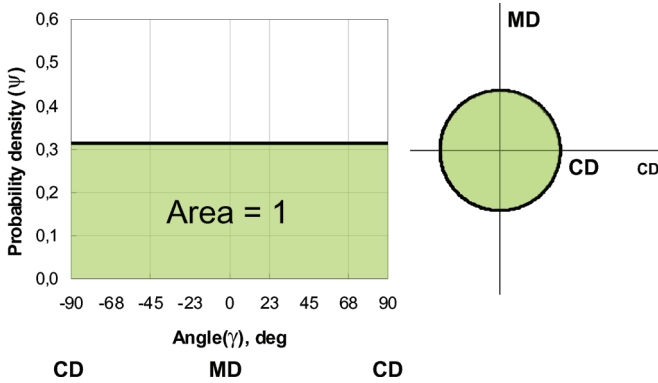


Figure 4. Probability density function for an isotropic paper (Equal number of fibres in all in-plane directions).

1- Cosine. – Corte and Kalmes (1962) used the 1- cosine term distributions according to Equation 3, where η_1 is a fitting parameter. It is based on a multi cosine term distribution introduced by Cox (1952).

$$\Psi(\gamma) = \frac{1}{\pi}(1 + \eta_1 \cos 2\gamma) \quad (3)$$

2- Cosine. – Perkins and Mark (1981) used the 2- cosine term distributions according to Equation 4. It is based on a multi cosine term distribution introduced by Cox (1952). η_1 and η_2 are fitting parameters.

$$\Psi(\gamma) = \frac{1}{\pi}(1 + \eta_1 \cos 2\gamma + \eta_2 \cos 4\gamma) \quad (4)$$

von Mises. – Perkins and Mark (1981) introduced the von Mises distribution for describing the fibre orientation distribution. The probability density function is given by Equation 5. The modified Bessel function, $I_0(\kappa)$, is tabulated in mathematical handbooks and κ is the fitting parameter.

$$\Psi(\gamma) = \frac{1}{\pi} \frac{e^{\kappa \cos 2\gamma}}{I_0(\kappa)} \quad (5)$$

Elliptical. – Prud’homme *et al.* (1975) used Equation 6 for the fibre orientation probability density function of paper. It was named “elliptical” by Perkins and Mark (1981) using C as a fitting parameter and given credit, but not explicitly given therein, to Forgacs and Strelis (1963).

$$\Psi(\gamma) = \frac{1}{\pi} \left(\frac{C}{\cos^2 \gamma + C^2 \sin^2 \gamma} \right) \quad (6)$$

Cauchy. – Schulgasser (1985) proposed the standard wrapped-up Cauchy distribution for describing fibre orientation distribution in paper. It is often used as an alternative to the Von Mises distribution for symmetric circular data. The probability density function is given in Equation 7 where p is the fitting parameter.

$$\Psi(\gamma) = \frac{1}{\pi} \frac{1-p^2}{1+p^2-2p \cos(2\gamma)} \quad (7)$$

Ellipse. – Christiansson and Lucisano (2004) states that they use an ellipse for describing the fibre orientation distribution. The probability density function for an ellipse can be defined according to Equation 8, where the major and minor axis of the ellipse a and b are fitting parameters.

$$\Psi(\gamma) = \frac{r}{\int_{-\pi/2}^{\pi/2} r \, d\gamma} \quad \text{where} \quad r = \frac{ab}{\sqrt{a^2 \sin^2 \gamma + b^2 \cos^2 \gamma}} \quad (8)$$

Equivalent pore. – Silvy (1980) described the fibre orientation distribution according to Equation 9 as a part of his “equivalent pore concept” where e is the excentricity, a the major and b the minor axis of an ellipse describing the “mean shape” of the projection of the pores in the paper structure. The fibre orientation distribution can be described using one measurable parameter, the fibre orientation anisotropy A_F (dimensionless).

$$\Psi(\gamma) = \frac{1}{\pi} \frac{1-e^2}{(1-f(e))(1-e^2 \sin^2(\gamma))^{3/2}} \quad \text{where} \quad f(e) = \sum_{k=1}^{\infty} \frac{e^{2k}}{2k-1} \left(\prod_{p=1}^k \left(\frac{2p-1}{2p} \right)^2 \right) \quad (9)$$

$$\text{and } e = \sqrt{1 - \left(\frac{b}{a} \right)^2} \quad \text{and} \quad \frac{a}{b} = \sqrt[3]{A_F}$$

Fibre orientation distributions – new derivations

Fluid mechanics. – Olson (2002) derived an analytical expression for the fibre orientation distribution after an arbitrary shaped headbox nozzle with the contraction ratio as parameter. In Appendix 1 it is shown that the contraction ratio in Olsons expression can be substituted with the square root of the fibre orientation anisotropy, A_F . Equation 10 with the fibre orientation anisotropy as a measurable parameter is proposed as an approximation for fibre orientation distribution in paper.

$$\Psi(\gamma) = \frac{1}{\pi} \frac{(1 + \tan^2 \gamma) \sqrt{A_F}}{1 + A_F \tan^2 \gamma} \quad (10)$$

Orthotropic analysis. – A probability density function according to Equation 11 is proposed as an approximation for fibre orientation distribution in paper. Equation 11 is based on classical textbook orthotropic analysis, a proposed equality between fibre orientation and stiffness distributions and simplified established approximations for paper. The measurable parameter A_F is the fibre orientation anisotropy of the paper. The derivation is described in detail in Appendix 2

$$\Psi(\gamma) = \frac{1}{\pi} \left(\frac{1}{\sqrt{A_F}} \cos^4 \gamma + 2 \sin^2 \gamma \cos^2 \gamma + \sqrt{A_F} \sin^4 \gamma \right)^{-1} \quad (11)$$

Stress/strain analysis. – A probability density function according to Equation 12 is proposed as an approximation for fibre orientation distribution in paper. Equation 12 is based on a simple Stress/strain analysis together with Hooke's law, a proposed equality between fibre orientation and stiffness distributions. The measurable parameter A_F is the fibre orientation anisotropy of the paper. The derivation is described in detail in Appendix 3 (Equation 50 to Equation 52).

$$\Psi(\gamma) = \frac{1}{\pi} \left(\frac{\sqrt{A_F}}{\cos^2 \gamma + A_F \sin^2 \gamma} \right) \quad (12)$$

Tensile stiffness distributions – previous work

Stress/strain analysis. – Equation 13 was proposed by Horio and Onogi (1951) as an approximation of tensile stiffness distribution in paper. It is often referred to as Hankinson's equation from a 1921 US Air Service investigation of spruce strength. It is based on a very simple Stress/strain analysis together

with Hooke's law. Although the analysis is outdated the derivation is included in Appendix 3 to give the complete picture of the derivation of Equation 12. The measurable parameters E_{MD} and E_{CD} are the MD and CD tensile stiffness index of the paper (MNm/kg).

$$E(\gamma) = \frac{E_{MD}E_{CD}}{E_{MD} \sin^2 \gamma + E_{CD} \cos^2 \gamma} \quad (13)$$

Tensile stiffness distributions – new derivations

Fluid mechanics. – Equation 14 is proposed as an approximation of tensile stiffness distribution in paper. The fibre orientation anisotropy, A_F and the isotropic tensile stiffness index, E_{Iso} , are the measurable parameters. Equation 14 is based on Equation 10 and an assumption that the normalised fibre orientation distribution is equal to the normalised tensile stiffness distribution for restrained dried paper. It is also proposed that Equation 14 can be generalised to be valid for any paper according to Equation 15 where the tensile stiffness index in MD and CD are measurable parameters. All derivations are given in detail in Appendix 1.

$$E^r(\gamma) = \frac{1 + \tan^2 \gamma}{1 + A_F \tan^2 \gamma} E_{Iso} \sqrt{A_F} \quad (14)$$

$$E(\gamma) = \frac{1 + \tan^2 \gamma}{1 + \frac{E_{MD}}{E_{CD}} \tan^2 \gamma} E_{MD} \quad (15)$$

Orthotropic analysis. – Equation 16 is proposed as an approximation of tensile stiffness distribution in paper. Equation 16 is based on classical orthotropic analysis and simplified established approximations for paper. The derivation is described in detail in Appendix 2 (Equation 38 to Equation 45). The measurable parameters are the tensile stiffness index in MD and CD in the paper.

$$E(\gamma) = \left(\frac{1}{E_{MD}} \cos^4 \gamma + \frac{2}{\sqrt{E_{MD}E_{CD}}} \sin^2 \gamma \cos^2 \gamma + \frac{1}{E_{CD}} \sin^4 \gamma \right)^{-1} \quad (16)$$

Relations between distribution functions

Sampson (2001) showed that substitution with $C = (p + 1)^2/(p - 1)^2$ in Equation 7 proposed by Schulgasser (1985) makes it identical to Equation 6

proposed by Prud'homme *et al.* (1975). If C in the distribution function proposed by Prud'homme *et al.* (1975) (Equation 6) is substituted with $\sqrt{A_F}$ the distribution function gives the same results as the Fluid mechanics based derivation (Equation 10) and is also identical to the Stress/strain analysis based distribution function (Equation 12). Therefore the fibre orientation distribution functions by Prud'homme *et al.* (1975), Schulgasser (1985) and the proposed derivations based on Fluid mechanics and Stress/strain analysis will be treated together in the following evaluation of predictive ability.

Wahlström and Mäkelä (2005) showed that the tensile stiffness anisotropy for restrained dried paper is equal to the fibre orientation anisotropy. A hypothesis put forward in this work is that this can be expanded to the normalised fibre orientation distribution being equal to the normalised tensile stiffness distribution for restrained dried (r) paper according to Equation 17 where $\gamma = 0 = MD$.

$$\frac{\Psi(\gamma)}{\Psi(\gamma=0)} = \frac{E^r(\gamma)}{E^r(\gamma=0)} \quad (17)$$

Invariance of the distribution functions

The geometric mean of a property measured in MD and CD ($\sqrt{MD \times CD}$) is widely used as a way to characterize paper performance. Schrier and Verseput (1967) found empirically that the geometric mean of Taber stiffness in MD and CD was constant with varying anisotropy. Htun and Fellers (1982) later refined this by showing experimentally that the geometric mean of E_{MD} and E_{CD} is constant (invariant) with varying fibre orientation anisotropy only if the drying restraints are not changed. They also found that, for restrained drying, the geometric mean of E_{MD} and E_{CD} is equal to the isotropic quantity. Although widely used and accepted within the paper industry the use of the geometric mean is lacking a theoretical base.

To give the geometric mean a theoretical base it will be shown that the mean value of the distribution functions for tensile stiffness proposed in this work is equal to the geometric mean of E_{MD} and E_{CD} . The mean value of a distribution function for tensile stiffness, \bar{E} , can be written according to Equation 18. An analytical solution of Equation 18 with $E(\gamma)$ according to the approximation based on Fluid mechanics (Equation 15) shows that the mean value is equal to the geometric mean of E_{MD} and E_{CD} (Equation 19). The same result was achieved analytically for the Stress/strain analysis and numerically for the Orthotropic analysis.

$$\bar{E} = \frac{\int_{-\pi/2}^{\pi/2} E(\gamma) d\gamma}{\int_{-\pi/2}^{\pi/2} d\gamma} \quad (18)$$

$$\bar{E} = \frac{\int_{-\pi/2}^{\pi/2} \frac{(1 + \tan^2 \gamma) E_{MD}}{1 + (E_{MD}/E_{CD}) \tan^2 \gamma} d\gamma}{\int_{-\pi/2}^{\pi/2} d\gamma} = \frac{\left[\sqrt{E_{MD} E_{CD}} \tan^{-1} \left(\sqrt{\frac{E_{MD}}{E_{CD}}} \tan \gamma \right) \right]_{-\pi/2}^{\pi/2}}{[\gamma]_{-\pi/2}^{\pi/2}} = \sqrt{E_{MD} E_{CD}} \quad (19)$$

It will also be shown that the derived distribution functions are invariant under certain circumstances and thereby follow the findings by Htun and Fellers (1982). It is however not meaningful to show this for the stiffness distribution functions directly since E_{MD} and E_{CD} are variables in the functions. But by considering the assumed equality between the stiffness and fibre orientation distributions (Equation 17) it is possible to instead evaluate the behaviour of the directly linked fibre orientation distributions.

If the geometric mean of $\Psi(\gamma = 0 = MD)$ and $\Psi(\gamma = \pi/2 = CD)$ is constant for varying fibre orientation anisotropy also the geometric mean of E_{MD} and E_{CD} should be constant, and for restrained drying equal to the isotropic stiffness (Equation 20).

$$E_{iso}^r = \sqrt{E_{MD}^r E_{CD}^r} \quad (20)$$

Varying fibre orientation anisotropy means redistribution of a given amount of fibres. Therefore the mean value of a distribution function for fibre orientation expressed as a probability density function must always be equal to the isotropic value $1/\pi$ (Equation 2). This can also be shown with the same type of derivation as in Equation 18 and Equation 19 but for fibre orientation. Thereby the assumed equality between stiffness and fibre orientation distributions gives that the mean value or geometric mean of E_{MD} and E_{CD} is equal to the isotropic stiffness at restrained drying. The behaviour of the geometric mean of $\Psi(\gamma = 0)$ and $\Psi(\gamma = \pi/2)$ with varying fibre orientation will be evaluated numerically to compare the discussed distribution functions with the findings by Htun and Fellers (1982).

Decoupling fibre orientation and drying restraints

To derive a description with the fibre orientation anisotropy and the total accumulated strain (shrinkage or stretch) during drying in MD and CD as adjustable parameters a description proposed by Wahlström and Mäkelä (2005) is applied. Equation 21 and Equation 22 describes a linear relation

between tensile stiffness index and total strain accumulated during drying, ε , for MD and CD respectively. ε (%) is the sum of shrinkage and stretch during drying. E^r is the restrained dried tensile stiffness, E^{fs} the freely dried tensile stiffness and ε^{fs} the free shrinkage strain (%), or shrinkage potential, for the same paper. Equation 23 to Equation 28 gives relations between the anisotropic (MD and CD) and the isotropic properties with fibre orientation anisotropy, A_F , as adjustable variable.

$$E_{MD} = E_{MD}^r - \frac{E_{MD}^r - E_{MD}^{fs}}{\varepsilon_{MD}^{fs}} \varepsilon_{MD} \cdot \quad (21)$$

$$E_{CD} = E_{CD}^r - \frac{E_{CD}^r - E_{CD}^{fs}}{\varepsilon_{CD}^{fs}} \varepsilon_{CD} \quad (22)$$

$$E_{MD}^r = E_{Iso}^r \sqrt{A_F} \quad (23)$$

$$E_{MD}^{fs} = E_{Iso}^{fs} \sqrt{2A_F - 1} \quad (24)$$

$$\varepsilon_{MD}^{fs} = \varepsilon_{Iso}^{fs} / \sqrt{A_F} \quad (25)$$

$$E_{CD}^r = E_{Iso}^r / \sqrt{A_F} \quad (26)$$

$$E_{CD}^{fs} = E_{Iso}^{fs} / \sqrt{2A_F - 1} \quad (27)$$

$$\varepsilon_{CD}^{fs} = \varepsilon_{Iso}^{fs} \sqrt{A_F} \quad (28)$$

Inserting Equation 23 to Equation 25 in Equation 21 and Equation 26 to Equation 28 in Equation 22 gives Equation 29 and Equation 30.

$$E_{MD} = E_{Iso}^r \sqrt{A_F} - \frac{E_{Iso}^r \sqrt{A_F} - E_{Iso}^{fs} \sqrt{2A_F - 1}}{\varepsilon_{Iso}^{fs} / \sqrt{A_F}} \varepsilon_{MD} \quad (29)$$

$$E_{CD} = \frac{E_{Iso}^r}{\sqrt{A_F}} - \frac{E_{Iso}^r / \sqrt{A_F} - E_{Iso}^{fs} / \sqrt{2A_F - 1}}{\varepsilon_{Iso}^{fs} \sqrt{A_F}} \varepsilon_{CD} \quad (30)$$

Equation 13, Equation 15 or Equation 16 with E_{MD} and E_{CD} according to Equation 29 and Equation 30 gives a description of $E(\gamma)$ as a function of E_{Iso}^r , E_{Iso}^{fs} , ε_{Iso}^{fs} , ε_{MD} , ε_{CD} and A_F . E_{Iso}^r , E_{Iso}^{fs} and ε_{Iso}^{fs} are physical parameters that for

example can be measured on laboratory handsheets. The fibre orientation anisotropy A_F and the total accumulated strain (%) in MD, ε_{MD} , and in CD, ε_{CD} , are also measurable physical parameters but in this context they will probably most often be used as adjustable variables in predictions. For example to study how the tensile stiffness distribution for a given furnish is changed with varying fibre orientation anisotropy and shrinkage or stretch.

RESULTS

Fibre orientation distributions

Fibre orientation distribution was measured on handsheets with three different anisotropies. To evaluate the predictive ability of the discussed probability density functions (Equation 3 to Equation 12) they were compared with experimental data. The comparison was made with the condition of fulfilling Equation 1 and to give the same anisotropy as the experimental data. The predictions and the experimental data were normalised to $\Psi(\gamma = 0) = 1$ by dividing $\Psi(\gamma)$ by $\Psi(\gamma = 0)$. All evaluated probability density functions are listed in Table 1 with the values of the parameters used in the predictions and the maximum deviation from the experimental data. The results are shown in Figure 5 to Figure 8 both in Cartesian coordinates and polar form. Using the polar form does not give any further insights, but is included since it is often used within paper physics. Figure 9 and Figure 10 show the deviation from the experimental data for the whole distribution. In the figures degrees are shown (-90 to 90) whereas in the calculations radians were used ($-\pi/2$ to $\pi/2$). The results for the handsheets with low anisotropy are not included since they were very close to an isotropic distribution and all evaluated functions gave the same result since they all can predict isotropic behaviour.

Tensile stiffness distributions

Varying fibre orientation anisotropy. – Tensile stiffness index distribution was measured on restrained dried handsheets with three different anisotropies. The distributions were predicted with the derivation based on fluid mechanics, Equation 14, and the Orthotropic analysis, Equation 44. The parameters used in both cases were the isotropic tensile stiffness $E_{Iso} = 7.11$ MNm/kg and the fibre orientation anisotropy $A_F = 1.06$ (**Red**), 1.68 (**Green**) and 2.92 (**Blue**). The coloured lines in Figure 11 and Figure 12 (see also Plates 30 and 31) refer to the Orthotropic analysis based predictions and the grey to the Fluid mechanics but also the Stress/strain based since they gave identical results. Circles

Table 1. Parameter values used in the predictions of fibre orientation distribution functions and maximum deviation of the predictions from experimental data. Legend for Figure 5 to Figure 10 and Figure 19.

Legend	Fibre orientation distribution functions	Parameter values		Max deviation	
		Medium	High A_F	Medium	High A_F
Circles	Experimental data	$A_F = 2.37$	$A_F = 4.03$	Reference	Reference
Grey	1-Cosine Equation 3 Corte and Kallmes (1962)	$\eta = 0.41$	$\eta = 0.60$	29%	50%
Red	2-Cosine Equation 4 Perkins and Mark (1981)	$\eta_1 = 0.44$ $\eta_2 = 0.09$	$\eta_1 = 0.75$ $\eta_2 = 0.25$	10%	-22%
Purple	Von Mises Equation 5 Perkins and Mark (1981)	$\kappa = 0.43$	$\kappa = 0.70$	19%	23%
Blue	Ellipse Equation 8 Christiansson and Lucisano (2004)	$a = 2.37$ $b = 1.00$	$a = 4.03$ $b = 1.00$	-7%	-24%
Turquoise	Equivalent pore concept Equation 9 Silvy (1980)	$A_F = 2.37$	$A_F = 4.03$	5%	11%
Black	Equation 6 Prud'homme <i>et al.</i> (1975), Equation 7 Schulgasser (1985), Equation 31 Akbar and Altan (1992)	$C = 1.54$ $p = 0.216$ $\varepsilon = 0.216$	$C = 2.01$ $p = 0.348$ $\varepsilon = 0.348$	8%	-7%
Black	Present work Equation 10 Fluid Mechanics, Equation 12 Stress/strain Analysis	$A_F = 2.37$	$A_F = 4.03$	8%	-7%
Green	Present work Equation 11 Orthotropic Analysis	$A_F = 2.37$	$A_F = 4.03$	13%	9%

in the respective colour are the experimental results. The isotropic tensile stiffness was calculated as the mean of the isotropic tensile stiffness for each paper calculated with Equation 19. The fibre orientation anisotropy was measured on each paper with the same method that was used for measuring the fibre orientation distribution. The maximum deviation of predicted tensile stiffness index from the measured tensile stiffness index (coloured circles) was up to around 10 % as shown in Figure 13 and Figure 14.

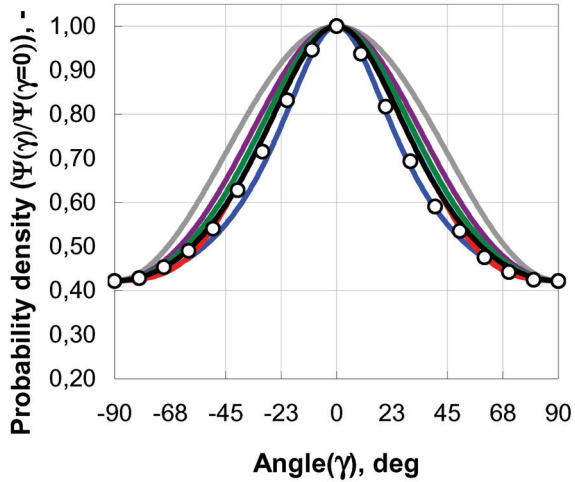


Figure 5. Measured and predicted fibre orientation distribution functions according to Table 1 for $A_F = 2.37$. Cartesian form.

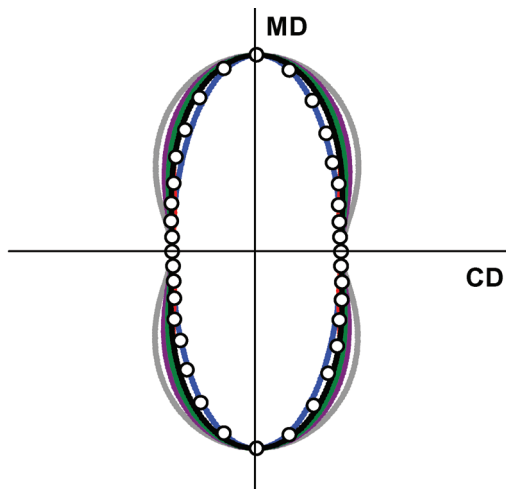


Figure 6. Measured and predicted fibre orientation distribution functions according to Table 1 for $A_F = 2.37$. Polar form.

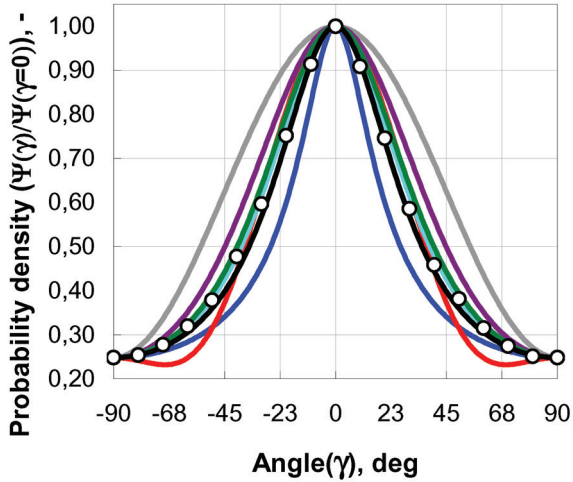


Figure 7. Measured and predicted fibre orientation distribution functions according to Table 1 for $A_F = 4.03$. Cartesian form.

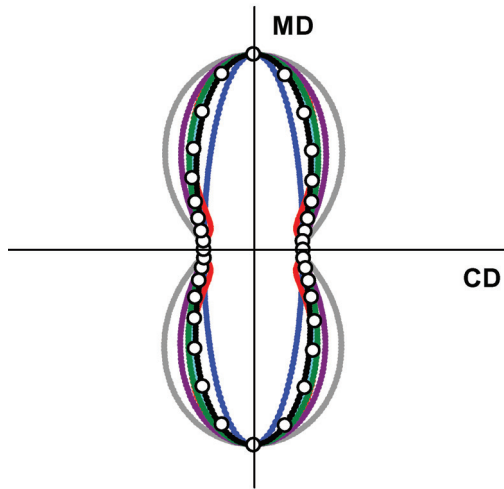


Figure 8. Measured and predicted fibre orientation distribution functions according to Table 1 for $A_F = 4.03$. Polar form.

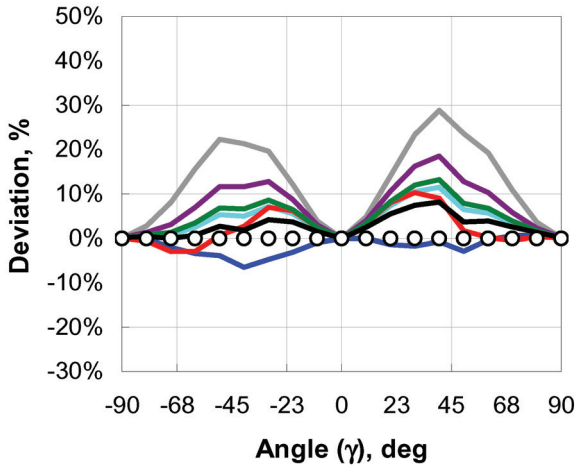


Figure 9. Deviation of the predicted fibre orientation distribution from the experimental data for $A_f = 2.37$.

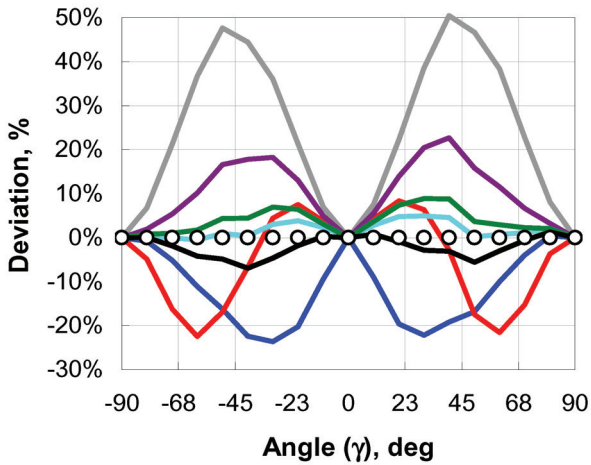


Figure 10. Deviation of the predicted fibre orientation distribution from the experimental data for $A_f = 4.03$.

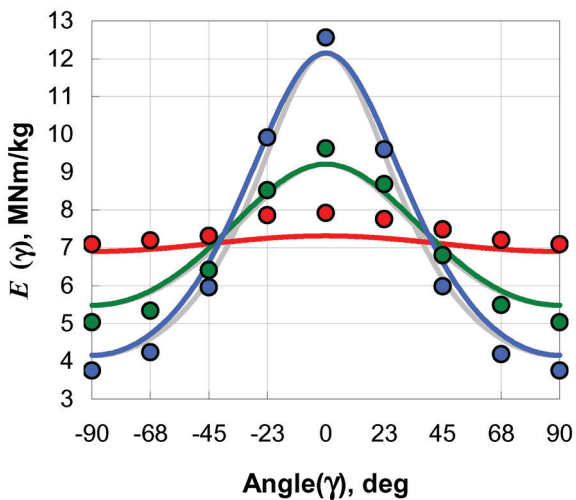


Figure 11. Measured and predicted tensile stiffness index distributions for varying fibre orientation anisotropy in Cartesian form.

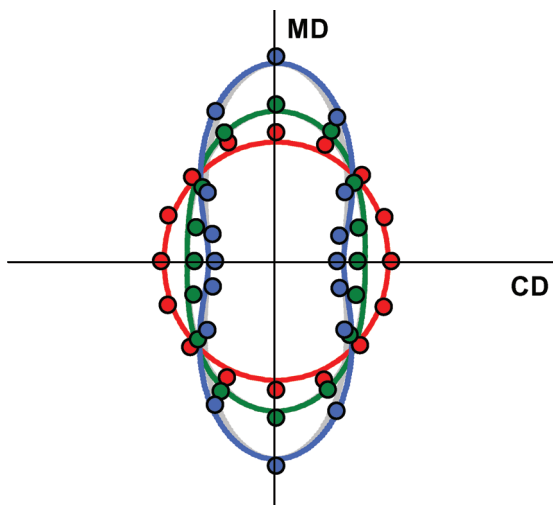


Figure 12. Measured and predicted tensile stiffness index distributions for varying fibre orientation anisotropy in polar form.

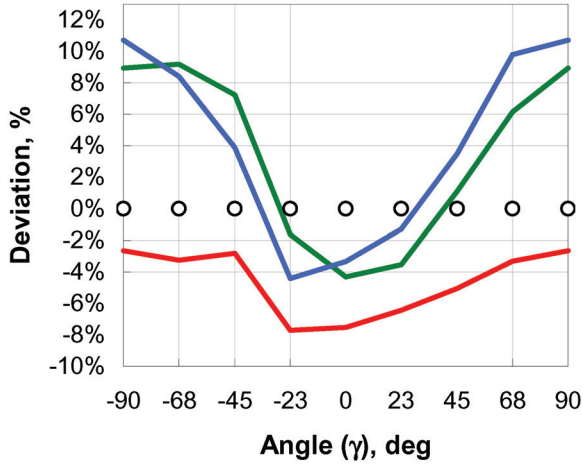


Figure 13. Deviation of predicted tensile stiffness index from measurements for the Fluid mechanics based approach.

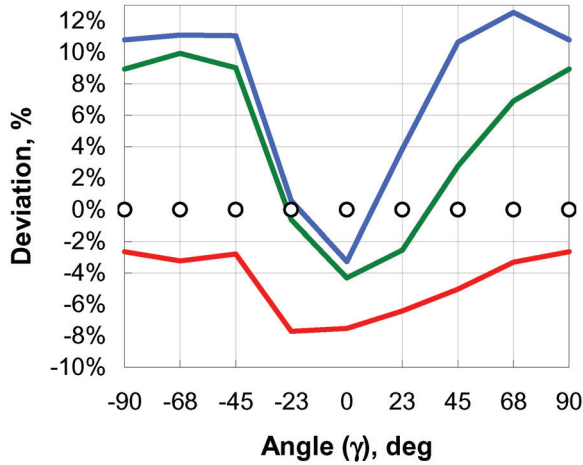


Figure 14. Deviation of predicted tensile stiffness index from measurements for the Orthotropic Analysis based approach.

Varying drying restraints. – The tensile stiffness index distribution was measured on paper dried with different drying restraints in MD and CD according to Table 2. The distributions were predicted using the Fluid mechanics based approach (Equation 15), the Orthotropic analysis (Equation 16) and the Stress/strain analysis (Equation 13). Parameters for predictions according to Table 2 were taken from the measurements. The experimental and predicted results are presented in Figure 15 and Figure 16. The coloured lines refer to

Table 2. Legend, parameters used in the predictions and maximum deviation from measurements for the distributions with varying drying restraints in Figure 15 to Figure 18.

Colour	MD Restraint	CD Restraint	Parameters (MNm/kg)		Max deviation	
			E (MD)	E (CD)	Fluid/Stress	Orthotropic
Red	Free	Free	9.03	2.99	- 7 %	- 2 %
Yellow	Free	Restrained	9.00	5.44	+ 6 %	+ 8 %
Green	Restrained	Free	12.39	3.10	-10 %	+ 2 %
Blue	Restrained	Restrained	12.28	5.50	+ 3 %	+ 7 %
Circles	Rest/ Free	Rest/ Free	-	-	Reference	Reference

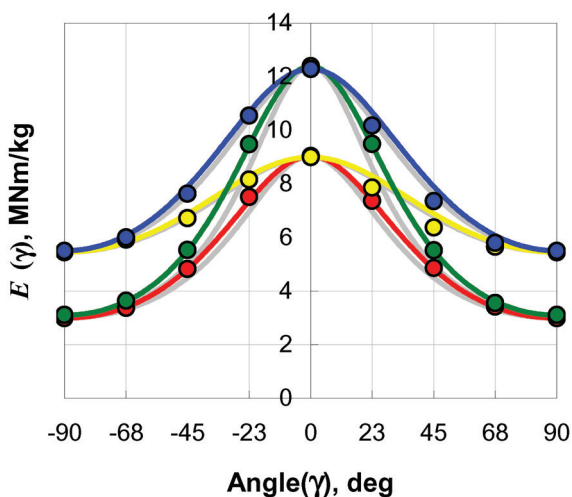


Figure 15. Measured and predicted tensile stiffness index distributions for varying drying restraints in MD and CD. Cartesian form.

the Orthotropic analysis based predictions and the grey to both the Fluid mechanics and Stress/strain based predictions since they gave identical results. Circles in the respective colour are the experimental results. Measured results were left out from Figure 16 to make it clearer. The deviation of the predicted stiffness from the measured stiffness is shown in Figure 17 and Figure 18.

Invariance of the distribution functions

To evaluate the invariance of the distribution functions the behaviour of the geometric mean of $\Psi(\gamma)$ in MD and CD are evaluated numerically with increasing fibre orientation. As discussed earlier the geometric mean or square root of $\Psi(\gamma)$ in MD times CD is equal to $1/\pi$ for the isotropic case ($A_f = 1$) and should be constant (invariant) with increasing fibre orientation anisotropy. Figure 19 shows the deviation of the geometric mean from the isotropic value ($1/\pi$) for all fibre orientation distribution functions included in this work (Legend according to Table 1). The distribution functions proposed by Prud'homme *et al.* (1975), Schulgasser (1985), Akbar and Altan (1992) and the approximations proposed in this work derived from Fluid Mechanics, Stress/strain Analysis and Orthotropic Analysis were all constant with increasing fibre orientation anisotropy. Whereas the approximations referred

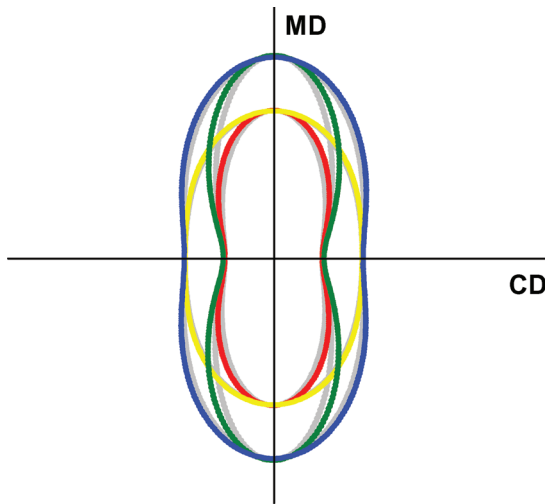


Figure 16. Predicted tensile stiffness index distributions for varying drying restraints in MD and CD. Polar form.

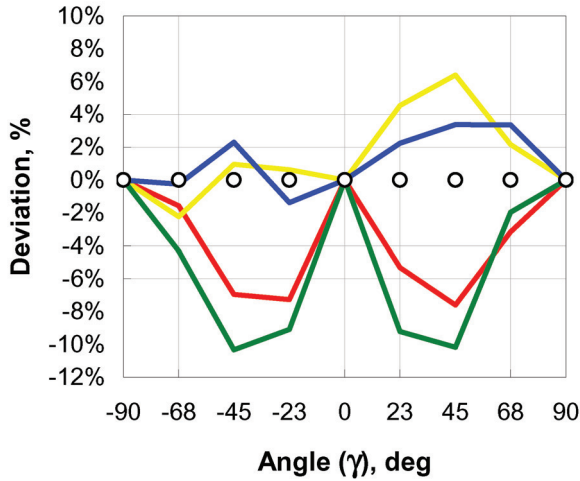


Figure 17. Deviation of predicted tensile stiffness from measurements for the Fluid mechanics and Stress/strain based approach.

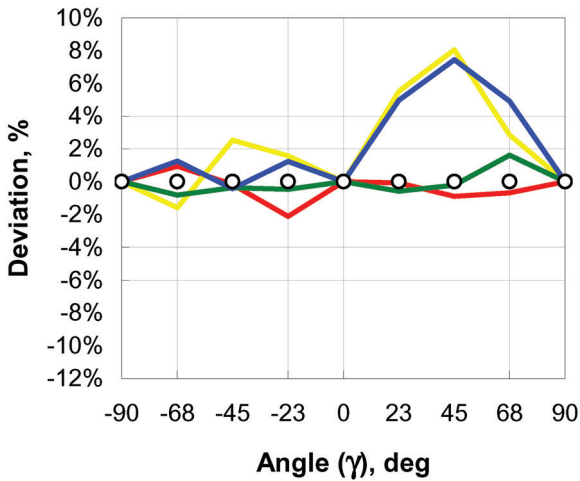


Figure 18. Deviation of predicted tensile stiffness from measurements for the Orthotropic analysis based approach.

to as the 1-Cosine, von Mises, Ellipse and Equivalent pore concept is not constant with increasing fibre orientation anisotropy. The 2-cosine distribution function does neither deviate from the geometric mean but it is not of interest since its two parameters were adjusted to fulfil the same condition.

DISCUSSION

The fluid mechanics based derivations – (Appendix 1) are based on Olson (2002) who derived a simplified function (Equation 32) for describing fibre orientation in an accelerating flow field using headbox contraction ratio (R) as controlling parameter. Olson assumed straight, rigid, infinitely thin and inertialess fibres, linear, incompressible, non-turbulent and one-dimensional flow and a fibre concentration low enough to avoid fibre to fibre interactions. Obviously these simplifications affect the fibre orientation distribution and several of them has also been addressed in later studies by the same author, for example the anisotropy reducing effect from turbulence (Olson *et al.* 2005) and fibre to fibre interactions (Krochak *et al.* 2007). Regardless of all these simplifications the found relation for substitution of R with the square root of A_F together with the relation derived by Olson (2002) is very useful for predictions of the fibre orientation distribution in paper based on A_F (Equation 10). With an assumption of equality between fibre orientation and

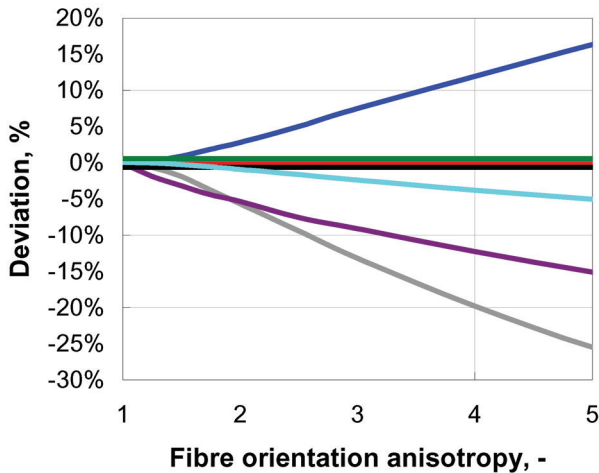


Figure 19. Deviation of the geometric mean from the isotropic value for the fibre orientation distribution functions listed in Table 1.

stiffness distribution it is also very useful for predictions of tensile stiffness distribution in paper (Equation 14). Note that the used description predicts the fibre orientation distribution based on the fibre orientation anisotropy in paper, A_F , not the furnish type, headbox geometry or the flow conditions in the headbox or the mix to forming fabric interaction etc. This means that the relation between R and A_F in Equation 33 is to be used only as a substitution to get a function based on a parameter that is measurable in paper. It is not a link between process and paper properties, that link is much more complicated. Also the fibre orientation anisotropy is known to vary over the thickness of the paper (Jansson 1999). The predictions in this work are made for the through thickness average fibre orientation distribution.

Akbar and Altan (1992) derived an analytical solution for rigid fibres in a dilute fibre suspension subjected to planar elongational flow from the equations of motion proposed by Jeffery *et al.* (1922). Their derived distribution function given by Equation 31 (with $\lambda = 1$ in their Equation 57) can be used for predictions of fibre orientation distribution in paper with ε (a measure of the elongation of the flow) as a fitting parameter. If ε is substituted with $\ln A_F / 4$ the distribution function gives the same results as the fluid mechanics based derivation (Equation 10).

$$\Psi(\gamma) = \frac{1}{\pi} \frac{1}{\cosh^2(\varepsilon) + \sinh^2(\varepsilon) - \sinh(2\varepsilon)\cos(2\gamma)} \quad (31)$$

Olson (2002) derived his equations from scratch but notes at one stage that they were identical to Jeffery *et al.* (1922). This common base may explain why they gave identical results. It may be possible to show that also the fitting parameters in Equation 31 (Akbar and Altan 1992) and Equation 6 (Prud'homme *et al.* 1975) can be treated as measurable physical parameters since they give identical results as Equation 10 (Olson 2002). However no attempt has been made in this work to carry out that analysis.

The orthotropic analysis based derivation – for tensile stiffness distribution (Appendix 2) are based on classical orthotropic analysis and simplified established approximations for paper. Baum *et al.* (1981) proposed the well known

approximation $\sqrt{v_{MDCD}v_{CDMD}} = 0.293$ and, by applying it in Equation 40, the

also well known $G_{MDCD} = 0.387 \sqrt{E_{MD}E_{CD}}$. If those approximations are applied on Equation 38 they give the same result as Equation 43 derived in this work. The value of Equation 38 is not dependent on the constant 0.293 for v_{iso} . Note also that neither v_{MDCD} nor G_{MDCD} is part of Equation 43. This does not mean that the distribution of tensile stiffness in paper is independent

of v_{MDCD} nor G_{MDCD} . Only that they vary together in such a way (Equation 40) that they can be excluded from Equation 38 in this proposed approximation for paper. For other purposes, such as predicting Poisson's ratio using Equation 42, the value of 0.293 for v_{iso} of course has to be used. Baum *et al.* (1981) refers Equation 40 to Szilard (1974). Note however that Szilard (1974) used this as a fact and do not give any background or reference to its origin.

The stress/strain analysis based derivation – for fibre orientation distribution (Appendix 3) are based on a very simple Stress/strain analysis together with Hooke's law and an assumed equality between fibre orientation and stiffness distribution. Since Prud'homme *et al.* (1975) does not give any background to the derivation or origin of Equation 6 it can be interesting to note that it gives the the same results as the Stress/strain analysis based distribution function if C is substituted with $\sqrt{A_F}$.

Relations between distribution functions. – Wahlström and Mäkelä (2005) showed that the tensile stiffness anisotropy for restrained dried paper is equal to the fibre orientation anisotropy. The hypothesis put forward in this work is that this can be expanded to the normalised fibre orientation distribution being equal to the normalised tensile stiffness distribution for restrained dried paper according to Equation 17. Based on this assumption the two distributions should have the same generic shape. The proposed link was evaluated by predicting the fibre orientation and tensile stiffness distribution based on the link. The analysis of the deviation of predicted results compared to measured showed a deviation of around 10% which is regarded as good for engineering purposes. Especially since there are some uncertainties in the measurements, for example the basis weight of each examined layer is not known which makes the averaging of the layers less perfect. Also the samples exhibited some skewness that was not corrected for. Other authors, for example Rigdahl *et al.* (1983), did not assume a 1:1 relation between fibre orientation and tensile stiffness orientation. When applying their hypothesis where the fourier coefficients are used as a link between fibre orientation and tensile stiffness (their Equation 14) the results show a large deviation to the experimental results achieved in this study. Adding a fitting parameter as in their Equation 17 would probably solve this but was not found to be an interesting alternative compared to the approaches studied here since it means using one extra not measurable parameter.

Decoupling fibre orientation and drying restraints. – Equation 29 and Equation 30 incorporates drying restraints in the proposed description and makes it possible to decouple the effect of fibre orientation and drying restraints respectively on tensile stiffness index. The validity of Equation 29 and

Equation 30 is discussed by Wahlström (2004) and by Wahlström and Mäkelä (2005). The independence of fibre anisotropy and shrinkage or stretch is often questioned. In addition to the discussion in Wahlström and Mäkelä (2005) Niskanen (1989) states that if an isotropic fibre network is strained ε % then the fibre orientation anisotropy is approximately equal to $1 + 0.015 \varepsilon$. Such a small change in fibre orientation anisotropy can be disregarded when it comes to having an effect on paper properties.

Fibre orientation. – The common understanding of the creation of fibre orientation in papermaking is that two different basic mechanisms are acting on the fibres: firstly, in the headbox nozzle contraction and, secondly, in the mix to forming fabric interaction. In the nozzle contraction the accelerating flow rotates the fibres and in the mix to forming fabric interaction one end of the fibre gets anchored in the filtered fibre mat and the other end is rotated by the shear field. The simple approaches proposed in this work seems to be well suited for describing the fibre orientation distribution in paper and it may be speculated upon why. One possible explanation is that the basic mechanism behind the fibre rotation is principally the same in the accelerating flow and in the shear flow, namely rotation due to different flow velocities at the different fibre ends. Figure 2 shows a fibre in an accelerating flow rotating in the MD/CD plane. Since the accelerating flow is symmetric the behaviour in the MD/ZD plane is exactly the same and the fibre rotates both in the MD/CD and the MD/ZD plane. Figure 1 shows a fibre rotating in a schematic shear field seen from a side view, in the MD/ZD plane, and also here the fibre will rotate. The different flow velocities at the different ends of the fibre can be due to either the shear flow or the anchoring in the fibre mat. Consider now a shear flow from above as shown in Figure 20. Also in the MD/CD plane the flow velocity differ at the different ends of the fibre, due to their difference in ZD position, and a rotation will take place. Figure 21 shows the flow and fibre from Figure 1 and Figure 20 in a 3- dimensional view and illustrates the mechanisms for rotation in both MD/ZD and MD/CD in a shear flow. Note that the illustrations of the flow fields are very simplified and only serves the purpose of illustrating the different flow velocity at the different ends of a fibre. In reality the shear flow in the mix to forming fabric interaction has a very strong gradient towards the filtered fibre mat and a more plug flow character in its bulk flow (Andersson and Bergström 1954). The anchoring effect has been shown for individual flocs (Bergstrom *et al.* 2003) but not for individual fibres.

Probability density functions. – The fibre orientation distribution functions are given as probability density functions in this work. A probability density function is often used for continuous random variables, such as orientation

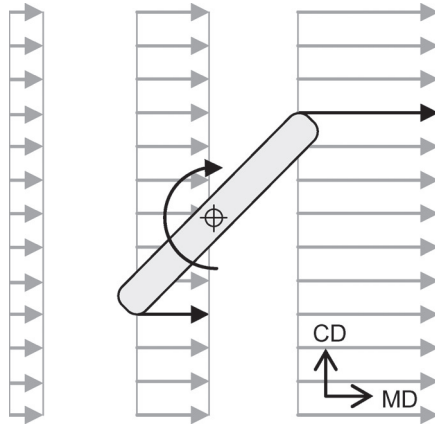


Figure 20. A fibre in a shear flow (schematic for mix to wire interaction) seen from above. Rotation in the MD/CD plane.

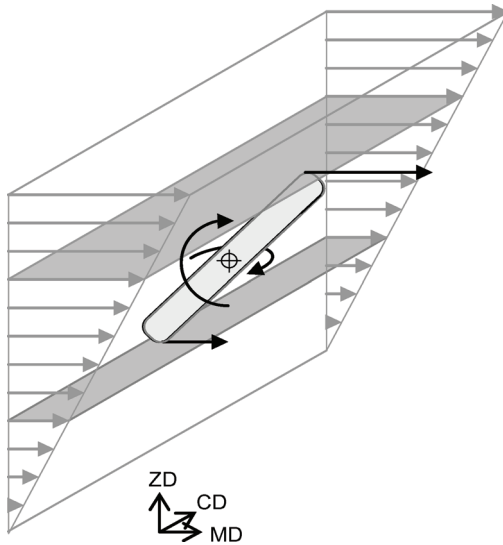


Figure 21. Three dimensional view of a fibre in a shear flow (schematic for mix to wire interaction). Rotation in MD/CD and MD/ZD.

angles. The probability that a fibre has an orientation of for example 45 degrees is zero, but the probability that a fibre has orientation between, for example, 44 and 46 degrees can be obtained by integrating the probability density between these values. A probability density functions can have values greater than 1, but probabilities cannot. In the present work the probability functions are normalised, the same functions not normalised are given as comparison in Figure 22. An alternative method not carried out in this work would have been to integrate the probability function to obtain the cumulative distribution function and then fit this to the cumulative data.

The peanut shape in paper. – Based on experimental and theoretical results the fibre orientation distribution in polar form has more of a “peanut” shape for high anisotropies (starting at $A > 2.0$) compared to a more elliptical shape at lower anisotropies (< 2.0). Machine made papers often shows a pronounced “peanut” shape for stiffness compared to the ones shown here for varying anisotropy and restrained drying. The explanation is that CD shrinkage of the paper reduces CD stiffness and thereby making the “peanut” shape stronger. This is very clear in the drying restraint part of this work for the sample with restrained drying in MD and free drying in CD. Also the sample with free drying in both MD and CD creates a peanut shape. This is due to that free shrinkage of the paper reduces CD stiffness relatively more com-

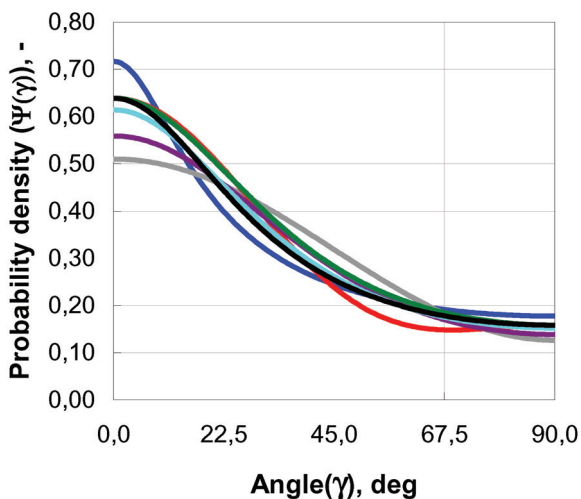


Figure 22. Not normalised fibre orientation distribution functions listed in Table 1 for $A_f = 4,03$.

pared to MD stiffness (Wahlström and Mäkelä 2005). Note however that there are no special physical mechanisms creating the waist in the “peanut shaped” distribution as is often discussed. As seen in this work the waist does not appear when the distributions are plotted in Cartesian form. It is only a consequence of plotting the distributions in polar form, nothing special happens in the transition point between “waist” and “no waist”. Most of us are accustomed to seeing results in Cartesian form and not in polar form and therefore may jump to conclusions. The distribution function in the left picture in Figure 23 ($A_F = 2$) gives the impression that the number of fibres does not change around the CD or $\Psi(\gamma = \pi/2)$, whereas in the right picture in Figure 23 ($A_F = 4$) it seems like there is an increase around the CD. Probably we base this assumption on the straight line that appears in the polar form for $A_F = 2$ but in reality they both increase and can be described with the same distribution function (with varying A_F). The “waist” appears if $\Psi(\gamma)$ is greater than the hypotenuse of a triangle with an adjacent equal to $\Psi(\gamma = \pi/2)$ for any γ . This condition is fulfilled when the fibre orientation anisotropy is above two, which can be understood from Figure 23. Note that the same condition is valid for the stiffness anisotropy (“waist” if $E_{MD}/E_{CD} > 2$), regardless of the combination of fibre orientation and drying restraint. Hopefully this rather awkward analysis shows the absurdity in the belief of a deeper meaning of the so called “peanut shape in paper”.

The skewness in paper – can also be incorporated in the distribution functions proposed in this work. Paper is said to exhibit a skewness if the maximum value of the fibre orientation or tensile stiffness distribution deviates from the

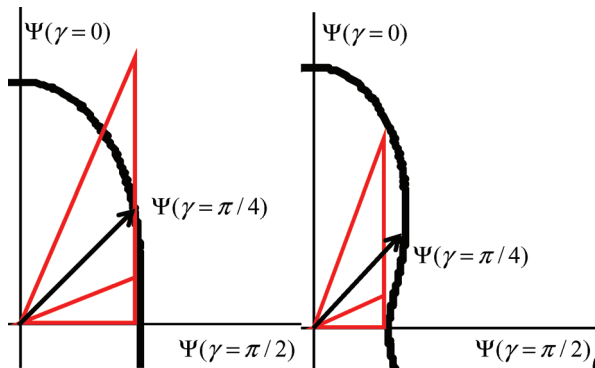


Figure 23. When the fibre orientation anisotropy is below two (left picture) no “waist” appears, but above two (right picture) a “waist” appears in a distribution function plotted in polar form.

MD. If the deviation in radians is defined as Δ the skewness can be included in the analysis made in this work by simply replacing γ with $\gamma + \Delta$. The distributions free-restrained and restrained- restrained in the drying restraint experiments obviously exhibited some skewness that could have been corrected for with this method but was not. Note that for just finding the skewness in paper it may not be necessary to use the distribution function that are best suited for predictions as was the purpose in this work. The best choice may for example be the distribution function that is easiest to fit to experimental data without the requirement of a fixed MD and CD value that was used in this work.

Choice of distribution functions. – Many different methods for measurements of fibre orientation distribution in paper have been published over the years, but there are no standards and measurements on the same papers have been shown to give different results (Perkins *et al.* 1983). One way to know that a measured fibre orientation distribution in paper is correct would be to link the measurements to some paper property that we have standardised methods for. In this work the normalised tensile stiffness distribution for restrained dried paper was proposed to be equal to the normalised fibre orientation distribution (Equation 17). The purpose with this work was to be able to predict distributions and therefore the predictive ability of the distribution functions has been evaluated. In practice this means they were all fitted to the same MD and CD values. Note that another purpose would have been to fit an equation to the experimental fibre orientation data without restricting the fit to the same MD and CD value. Then some of the curve fitting type of fibre orientation distribution functions dealt with (Equation 3 to Equation 8) or another function may have been as good or even better than the physical based functions since a polynomial or Fourier series with enough constants can naturally fit almost anything. Then the purpose however is not prediction and that analysis has therefore not been carried out in this work. Based on analysing the deviation from the experimental data the derived physical based functions performed best for the purpose of predictions among the distribution functions studied in this work. The maximum deviation was around 10% which is regarded as good for engineering purposes. The physical based functions also obeyed the condition of a constant geometric mean with varying fibre orientation anisotropy. An important strength is also that the used parameter or parameters are physically measurable on the paper. Considering this and the experimental results in this work the Orthotropic analysis based approach is the best choice for predictions.

CONCLUSIONS

The fibre orientation distribution in paper can be predicted by a function with one measurable physical parameter (The Fibre orientation anisotropy).

The tensile stiffness orientation distribution in paper can be predicted by a function with two measurable physical parameters (The Tensile stiffness in MD and CD).

The best predictions were achieved with the approach referred to as Orthotropic analysis in this work. This means that the studied paper behaviour follows classical orthotropic behaviour with some simplifications.

The normalised fibre orientation distribution is equal to the normalised tensile stiffness distribution for restrained dried paper. With this link the influence from fibre orientation and drying restraints on tensile stiffness can be decoupled.

The geometric mean or square root of MD times CD tensile stiffness is equal to the mean value of the tensile stiffness distribution function.

The waist in the “Peanut shape of paper” has no physical meaning.

ACKNOWLEDGEMENTS

Thanks to John Considine (FPL) for the suggestion to include an Orthotropic analysis approach and to Fredrik Thuvander (Karlstad University) for tutoring me in the same area. Thanks to Fredrik Thuvander, David Vahey (FPL), Paul Krochak (UBC) and Jacques Silvy (INP) for substantial discussions on various aspects of the work. Thanks to Bill Sampson (University of Manchester), Sören Östlund (KTH/Innventia), Petri Mäkelä (Innventia) and the FRC reviewers for valuable comments.

REFERENCES

- Akbar and Altan (1992) “On the solution of fiber orientation in two-dimensional homogenous flows” *Polymer engineering and science*, 32(12) 810–822.
- Andersson, O. and J. Bergström (1954) “Influence of differential speeds between stock and wire on sheet properties” *Tappi* 37(11):542–546.
- Baum, G.A., D.C. Brennan and C.C. Habeger (1981) “Orthotropic elastic constants of paper” *Tappi* 64(8): 97–101.
- Bergstrom, R., K. Åkesson and B. Norman (2003) “Floc behaviour in twin wire forming” PAPTAC 03.
- Christiansson, H. and M. Lucisano (2004) “Local fibre orientation in sheet layers” Fact sheet from STFi- Packforsk.

- Corte, H. and O.J. Kallmes (1962) "Statistical geometry of a fibrous network" In "Formation and structure of paper" (F. Bolam, Ed.), Tech. Sect. Brit. Paper & board makers' Assn., Vol 1, pp.13–46.
- Cox, H.L. (1952) Br. J. Appl. Phys. 3:72–79.
- Forgacs, O.L. and I. Strelis (1963) "The measurement of the quantity and orientation of chemical pulp fibres in the surfaces of newsprint" Pulp Paper Mag. Canada, 64:T-3–13.
- Horio, M. and S. Onogi. (1951) J. Appl. Phys. 22, 7, July, pp 971.
- Htun, M. and C. Fellers. (1982) "The invariant mechanical properties of oriented handsheets". Tappi Journal, 65 (4): 113–117.
- Hull, D. "Laminate theory" Chapter 6 in *An introduction to composite materials*, Cambridge solid state science series, Cambridge university press, p 102–110.
- Hyensjö, M. (2008) "Fibre orientation modelling applied to contracting flows related to papermaking" Doctoral thesis, The royal institute of technology, Department of mechanics, Stockholm, Sweden.
- Hämäläinen, T. and J. Hämäläinen (2007) "Modelling of fibre orientation in the headbox jet" Journal of pulp and paper science, 31(1), 49–53.
- Jansson, M. (1999) "Fiberriktninganisotropi – variationer i z-led", Master thesis, KTH, Stockholm, Sweden.
- Jeffery (1922) "The motion of ellipsoidal particles immersed in a viscous fluid" Proc. Royal Soc. Ser. A, 102, pp. 161–179.
- Jäsberg, A. (2007) "Flow behaviour of fibre suspensions in straight pipes: new experimental techniques and multiphase modeling" PhD thesis, University of Jyväskylä, Finland.
- Krochak, P.J., J.A. Olson and D.M. Martinez (2007) "Modeling the Orientation State of a Pulp Suspension in a Linear Contraction Headbox: The effect of fiber-fiber interactions" Tappi.
- Krochak, P. (2008) "The orientation of semi-dilute rigid fibre suspensions in a linearly contracting channel" Doctor of Philosophy Thesis, Mechanical Engineering, The University Of British Columbia, Vancouver.
- Lin(d)blad, G. (1996) "Using ultrasonic to predict compression strength". Paper Asia, August 1996, pp. 30–33.
- Lindstöm, S.B. and T. Uesaka (2008) "Particle-level simulation of forming of the fiber network in papermaking" International Journal of Engineering Science, 46 (2008) 858–876.
- Niskanen, K.J. (1989) "Distribution of fibre orientations in paper" in Fundamentals of papermaking (C.F. Baker and V.W. Punton, eds) Mech. Eng. Publ., London, 1989, vol 1, pp 275.
- Olson, J.A. (2002) "Analytic estimate of the fibre orientation distribution in a headbox flow" Nordic pulp and paper research journal, vol 17 no 3.
- Olson, J.A., I. Frigaard, C. Candice and J.P. Hämäläinen (2004) "Modeling a turbulent fibre suspension flowing in a planar contraction: The one-dimensional headbox" International Journal of Multiphase Flow 30 (2004) 51–66.
- Parsheh, M., M.L. Brown and C.K. Aidun (2005) "On the orientation of stiff fibres

- suspended in turbulent flow in a planar contraction” *J. Fluid Mech.* (2005), vol. 545, pp. 245–269.
- Perkins, R.W and R.E. Mark (1981) “Some new concepts of the relation between fibre orientation, fibre geometry and paper properties” In the Role of fundamental research in paper making, *Trans. Symp. 1981, Mech. Eng. Publ. Ltd., London*, 1983, pp. 479–525
- Perkins, R.W., R.E. Mark, J. Silvy, H. Andersson, A.R.K Eusufzai (1983) “Effects of fiber orientation distribution on the mechanical properties of paper” International paper physics conference, Harwichport, MA, September 18–22, 1983, pp. 83–87.
- Prud’homme, R.E., N.V. Hien, J. Noah and R.H. Marchessault (1975) “Determination of fiber orientation of cellulosic samples by x-ray diffraction” *J. Appl. Polymer. Sci.* 19, 2609.
- Rigdahl, M., H. Andersson, B. Westerlind and H. Hollmark (1983) “Elastic behaviour of low density paper described by network mechanics” *Fibre Sci. Technol.* 19(2): 127–144.
- Rigdahl, M. and H. Hollmark (1986) “Network mechanics” in: *Paper Structure and Properties* (J.A. Bristow and P. Kolseth editors). Marcel Dekker, New York, Basel. Chapter 12, pp 241–261.
- Sampson, W.W. (2001) “The structural characterisation of fibre networks in paper-making processes- a review” In *proc. The science of papermaking* (C.F. Baker, ed.), *Trans 12th Fund. Res. Symp.*, pp 1205–1288, FRS, Manchester, 2001.
- Schrier, B., and H. Verseput (1967) “Evaluating the performance of folding cartons” *Tappi* 50 (3): 114.
- Silvy, J. (1980) “Etude structurale de milieux fibreux”, Thèse de Doctorat d’Etat, Université Scientifique et Médicale et Institut Polytechnique de Grenoble (1980) Chap. II.
- Szilard, R. (1974) “Theory and analysis of plates” Prentice- Hall Inc., Englewood Cliffs, N.J.
- Wahlström, T., C. Fellers and M. Htun (2000) “A laboratory method for biaxial straining of paper during drying”. *Tappi Journal*, 83 (7): 75.
- Wahlström, T. (2004) “The invariant shrinkage and stiffness of paper, -modeling anisotropic behavior based on isotropic handsheets” *The 2004 progress in paper physics seminar*, June 21–24, 2004, NTNU and PFI, Trondheim, Norway, pp 105–108.
- Wahlström, T. and P. Mäkelä (2005) “Predictions of anisotropic multiply board properties based on isotropic ply properties and drying restraints” *The thirteenth Fundamental Research Symposium “Advances in Paper Science and Technology”* 11th–16th September 2005 in Cambridge, UK.

APPENDIX 1

DERIVATIONS BASED ON FLUID MECHANICS

Fibre Orientation Distribution. – Olson (2002) derived an analytical expression for the fibre orientation distribution of fibres after an arbitrary shaped headbox nozzle (Equation 32). It will be shown that the contraction ratio, R , in Equation 32 can be replaced by the square root of the fibre orientation anisotropy, A_F , in a paper giving a distribution function with one measurable physical parameter (Equation 34).

$$\Psi(\gamma) = \frac{1}{\pi} \frac{(1 + \tan^2 \gamma)R}{1 + R^2 \tan^2 \gamma} \quad (32)$$

The fibre orientation anisotropy is here defined as the ratio of the amount of fibres in MD and CD. With the terminology used in this work the anisotropy can be written as the ratio of the probability density function with $\gamma = 0$ (MD) and $\gamma = \pi/2$ (CD). Inserting $\gamma = 0$ and $\gamma = \pi/2$ respectively in Equation 32 gives

$$\Psi(\gamma = 0) = \frac{1}{\pi} \frac{(1 + \tan^2 0)R}{1 + R^2 \tan^2 0} = \frac{1}{\pi} \frac{(1+0)R}{1+0} = \frac{R}{\pi}$$

and

$$\Psi(\gamma = \frac{\pi}{2}) = \left[\frac{1}{\pi} \frac{\tan^2 \gamma}{\tan^2 \gamma} \frac{(1/\tan^2 \gamma + 1)R}{(1/\tan^2 \gamma + R^2)}, \left\{ \frac{1}{\tan^2 \gamma} \Rightarrow 0; \gamma \Rightarrow \frac{\pi}{2} \right\} \right] = \frac{1}{\pi} \frac{(0+1)R}{0+R^2} = \frac{1}{R\pi}$$

Thereby the fibre orientation anisotropy is

$$A_F = \frac{\Psi(\gamma = 0)}{\Psi(\gamma = \pi/2)} = \frac{R/\pi}{1/R\pi} = R^2 \quad (33)$$

and Equation 32 can be written as Equation 34.

$$\Psi(\gamma) = \frac{1}{\pi} \frac{(1 + \tan^2 \gamma)\sqrt{A_F}}{1 + A_F \tan^2 \gamma} \quad (34)$$

Tensile Stiffness Distribution. – Equation 34 can be expanded to a tensile stiffness distribution by using the hypothesis put forward in this work that the

normalised fibre orientation distribution is equal to the normalised tensile stiffness distribution for restrained dried paper. Equation 17 with Equation 34 gives Equation 35.

$$\begin{aligned}
 E^r(\gamma) &= \left(\frac{1}{\pi} \frac{(1 + \tan^2 \gamma) \sqrt{A_F}}{1 + A_F \tan^2 \gamma} \bigg/ \frac{1}{\pi} \frac{(1 + \tan^2 0) \sqrt{A_F}}{1 + A_F \tan^2 0} \right) E_{MD}^r \\
 &= \left(\frac{1}{\pi} \frac{(1 + \tan^2 \gamma) \sqrt{A_F}}{1 + A_F \tan^2 \gamma} \bigg/ \sqrt{A_F} \right) E_{MD}^r \Rightarrow E^r(\gamma) = \frac{1 + \tan^2 \gamma}{1 + A_F \tan^2 \gamma} E_{MD}^r
 \end{aligned} \tag{35}$$

Wahlström and Mäkelä (2005) showed that, for restrained dried papers, the tensile stiffness in the machine direction ($\gamma = 0$) can be expressed as a function of the isotropic tensile stiffness and the fibre orientation anisotropy (Equation 23). Equation 35 with Equation 23 gives the tensile stiffness distribution for restrained dried paper for a given isotropic tensile stiffness (restrained dried) and the fibre orientation anisotropy as adjustable parameter (Equation 36).

$$E^r(\gamma) = \frac{1 + \tan^2 \gamma}{1 + A_F \tan^2 \gamma} E_{iso}^r \sqrt{A_F} \tag{36}$$

A generalisation of the derived function for tensile stiffness distribution (Equation 35) valid for all papers is proposed without theoretical back up. The fibre orientation anisotropy, A_F , is substituted with the tensile stiffness anisotropy of the paper, E_{MD}/E_{CD} , and the restrained dried tensile stiffness in MD, E_{MD}^r , with the tensile stiffness in MD, E_{MD} , giving Equation 37.

$$E(\gamma) = \frac{1 + \tan^2 \gamma}{1 + \frac{E_{MD}}{E_{CD}} \tan^2 \gamma} E_{MD} \tag{37}$$

APPENDIX 2

DERIVATIONS BASED ON ORTHOTROPIC ANALYSIS

Tensile Stiffness Distribution. – Equation 38 is an expression of the Young’s modulus at any in-plane angle for an orthotropic material according to Orthotropic analysis (Hull 1981). In this work E is the tensile stiffness index, G the shear stiffness index and v_{MDCD} a function of the strain in CD when the paper is stretched in MD ($v_{MDCD} = -\varepsilon_{CD}/\varepsilon_{MD}$).

$$E(\gamma) = \left(\frac{1}{E_{MD}} \cos^4 \gamma + \left(\frac{1}{G_{MDCD}} - \frac{2\nu_{MDCD}}{E_{MD}} \right) \sin^2 \gamma \cos^2 \gamma + \frac{1}{E_{CD}} \sin^4 \gamma \right)^{-1} \quad (38)$$

Baum *et al.* (1981) proposed the well known approximation $\sqrt{\nu_{MDCD}\nu_{CDMD}} = 0.293$ for Poisson's ratio in paper. In line with the theoretical analysis earlier in this work regarding the mean value of a distribution as an invariant property of paper this approximation is simplified by proposing that the geometric mean of the in-plane Poisson's ratios is not a constant (0.293) but a measurable physical parameter, the isotropic Poisson's ratio according to Equation 39. Szilard (1974) used this approximation for orthotropic materials in the form of Equation 40. It can be noted that he did not give any reference to its origin or derivation. Equation 40 can be derived from the isotropic relation $G = E_{Iso}/2(1 + \nu_{Iso})$ together with Equation 20 and Equation 39. Since the derivation of Equation 40 includes Equation 20 it should be valid only for restrained dried papers, but without further theoretical back up it is generalized to any drying restraint.

$$\sqrt{\nu_{MDCD}\nu_{CDMD}} = \nu_{Iso} \quad (39)$$

$$G_{MDCD} = \frac{\sqrt{E_{MD}E_{CD}}}{2(1 + \sqrt{\nu_{MDCD}\nu_{CDMD}})} \quad (40)$$

$$\frac{\nu_{MDCD}}{E_{MD}} = \frac{\nu_{CDMD}}{E_{CD}} \quad (41)$$

The proposed approximation makes it possible to derive a simplified tensile stiffness distribution function (Equation 43). Equation 41 from classical Orthotropic analysis (Hull 1981) with Equation 39 gives Equation 42.

$$\nu_{MDCD} = \nu_{Iso} \sqrt{E_{MD}/E_{CD}} \quad (42)$$

Equation 38 can now be simplified by inserting the proposed approximations according to Equation 40 and Equation 42 which gives Equation 43 that can be used to predict $E(\gamma)$ with E_{MD} and E_{CD} as measurable physical variables.

$$E(\gamma) = \left(\frac{1}{E_{MD}} \cos^4 \gamma + \frac{2}{\sqrt{E_{MD}E_{CD}}} \sin^2 \gamma \cos^2 \gamma + \frac{1}{E_{CD}} \sin^4 \gamma \right)^{-1} \quad (43)$$

Equation 43 can also be used together with E_{MD} and E_{CD} according to Equation 29 and Equation 30 giving a description of $E(\gamma)$ as a function of E_{Iso}^r , E_{Iso}^{fs} , ε_{Iso}^{fs} , ε_{MD} , ε_{CD} and A_F as discussed earlier.

Fibre Orientation Distribution. – A probability density function for fibre orientation distribution is derived based on Equation 43. Substitution of E_{MD} and E_{CD} according to Equation 23 and Equation 26 (valid for restrained dried paper) in Equation 43 gives Equation 44.

$$E^r(\gamma) = E_{Iso}^r \left(\frac{1}{\sqrt{A_F}} \cos^4 \gamma + 2 \sin^2 \gamma \cos^2 \gamma + \sqrt{A_F} \sin^4 \gamma \right)^{-1} \quad (44)$$

The normalised probability density function is proposed to be equal to the normalised tensile stiffness distribution for restrained dried paper (Equation 17). By normalising with the isotropic values Equation 17 together with Equation 2 can be written as

$$\frac{\Psi(\gamma)}{\Psi_{Iso}(\gamma)} = \frac{E^r(\gamma)}{E_{Iso}^r(\gamma)} \Rightarrow \Psi(\gamma) = \frac{1}{\pi} \frac{E^r(\gamma)}{E_{Iso}^r}$$

which together with Equation 44 gives the probability density function according to Equation 45.

$$\Psi(\gamma) = \frac{1}{\pi} \left(\frac{1}{\sqrt{A_F}} \cos^4 \gamma + 2 \sin^2 \gamma \cos^2 \gamma + \sqrt{A_F} \sin^4 \gamma \right)^{-1} \quad (45)$$

APPENDIX 3

DERIVATIONS BASED ON STRESS/STRAIN ANALYSIS

Tensile Stiffness Distribution. – Horio and Onogi (1951) made a very simple and today outdated Stress/strain analysis which together with Hooke's law gives an expression that can be used to predict $E(\gamma)$ with E_{MD} and E_{CD} as measurable physical variables. The analysis (Equation 46 to Equation 49) is included here with the purpose to give the complete picture of the derivation of Equation 12 (Equation 52).

If a tension σ_γ is applied at an angle γ to MD according to Figure 24 the deformations in MD and CD are

$$\varepsilon_{MD} = \frac{\sigma_{MD}}{E_{MD}} = \frac{\sigma_\gamma \cos \gamma}{E_{MD}} \quad (46)$$

$$\varepsilon_{CD} = \frac{\sigma_{CD}}{E_{CD}} = \frac{\sigma_{\gamma} \sin \gamma}{E_{CD}} \quad (47)$$

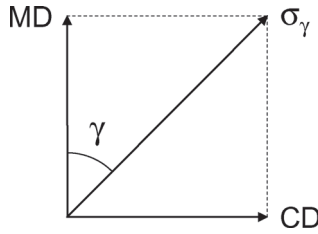


Figure 24. A tension σ_{γ} applied at an angle γ to MD.

The deformation, ε_{γ} , at an angle γ to MD according to Figure 25 can be expressed as

$$\varepsilon_{\gamma} = \varepsilon_{MD} \cos \gamma + \varepsilon_{CD} \cos(\pi/2 - \gamma) = \varepsilon_{MD} \cos \gamma + \varepsilon_{CD} \sin \gamma \quad (48)$$

Equation 48 with Equation 46 and Equation 47 gives $E(\gamma)$ with E_{MD} and E_{CD} as measurable physical variables (Equation 49).

$$\varepsilon_{\gamma} = \frac{\sigma_{\gamma} \cos \gamma}{E_{MD}} \cos \gamma + \frac{\sigma_{\gamma} \sin \gamma}{E_{CD}} \sin \gamma \Rightarrow [\sigma_{\gamma} = E_{\gamma} \varepsilon_{\gamma}] \Rightarrow \frac{1}{E_{\gamma}} = \frac{\cos^2 \gamma}{E_{MD}} + \frac{\sin^2 \gamma}{E_{CD}} \Rightarrow \quad (49)$$

$$E_{\gamma} = \frac{E_{MD} E_{CD}}{E_{MD} \sin^2 \gamma + E_{CD} \cos^2 \gamma}$$

Fibre Orientation Distribution. – Wahlström and Mäkelä (2005) showed that the tensile stiffness (E) anisotropy for restrained dried (r) paper is equal to the fibre orientation anisotropy, A_F , according to Equation 50.

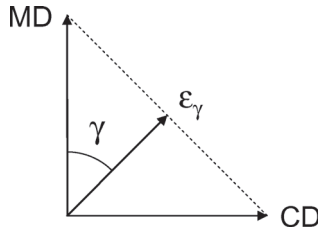


Figure 25. The deformation ε_{γ} at an angle γ to MD.

$$A_F = \frac{E_{MD}^r}{E_{CD}^r} \quad (50)$$

The normalised probability density function is proposed to be equal to the normalised tensile stiffness distribution for restrained dried paper (Equation 17). By instead normalising with the isotropic values Equation 17 together with Equation 2 gives Equation 51.

$$\frac{\Psi(\gamma)}{\Psi_{Iso}(\gamma)} = \frac{E^r(\gamma)}{E_{Iso}^r(\gamma)} \Rightarrow \Psi(\gamma) = \frac{1}{\pi} \frac{E^r(\gamma)}{E_{Iso}^r} \quad (51)$$

Equation 51 with Equation 26, Equation 50 and Equation 49 gives

$$\begin{aligned} \Psi(\gamma) &= \frac{1}{\pi} \frac{E^r(\gamma)}{E_{CD}^r \sqrt{A_F}} = \frac{1}{\pi} \frac{E^r(\gamma)}{E_{CD}^r \sqrt{E_{MD}^r/E_{CD}^r}} = \frac{1}{\pi} \frac{1}{\sqrt{E_{MD}^r E_{CD}^r}} \frac{E_{MD}^r E_{CD}^r}{E_{MD}^r \sin^2 \gamma + E_{CD}^r \cos^2 \gamma} = \\ &= \frac{1}{\pi} \frac{1}{\sqrt{E_{MD}^r E_{CD}^r}} \frac{E_{MD}^r}{(E_{MD}^r/E_{CD}^r) \sin^2 \gamma + \cos^2 \gamma} = \frac{1}{\pi} \frac{\sqrt{E_{MD}^r/E_{CD}^r}}{(E_{MD}^r/E_{CD}^r) \sin^2 \gamma + \cos^2 \gamma} \end{aligned}$$

And with Equation 50

$$\Psi(\gamma) = \frac{1}{\pi} \left(\frac{\sqrt{A_F}}{\cos^2 \gamma + A_F \sin^2 \gamma} \right) \quad (52)$$

Which with the substitution $C = \sqrt{A_F}$ is equal to the elliptical fibre orientation distribution function in Equation 6 proposed by Prud'homme *et al.* (1975). This alternative formulation however has the advantage of having the fibre orientation anisotropy of the paper, A_F , as a physical measurable parameter.

Transcription of Discussion

PREDICTION OF FIBRE ORIENTATION AND STIFFNESS DISTRIBUTIONS IN PAPER – AN ENGINEERING APPROACH

Torbjörn Wahlström

Stora Enso AB, Publication Paper R&D, Box 9090, 650 09 Karlstad, Sweden

Jari Hämäläinen University of Kuopio

What happens to your equation if there are not any fibres in the direction + or -90° to the MD? So the peanut's waist goes to zero. Sometimes in fluid mechanical fibre orientation, if we measure their orientation, there are hardly any fibres in this cross-machine direction, they are mostly oriented in the flow direction.

Torbjörn Wahlström

The equations cannot represent that case. Also, I have seen that the proposed equality holds up to a fibre orientation anisotropy of around 4. We will never get higher anisotropy than 4 in paper, so it is not a problem to apply the equations to paper as I do.

Ulrich Hirn Graz University of Technology

Tensile stiffness measurement is also well established as an indicator of the fibre orientation angle and anisotropy, and it seems that you always have this problem – that it measures the shrinkage and fibre orientation. My question is, if you measure the elastic modulus, can you directly derive the true fibre orientation from the tensile stiffness orientation measurements?

Discussion

Torbjörn Wahlström

Not if you take a real paper sample, because you do not know how much stretch or shrinkage there is in the paper. Hess and Brodeur (JPPS 22(5) pp. J160–164, 1996) showed that tensile stiffness orientation is changed by wet straining and shrinkage, whereas fibre orientation angle is not. But for optimization of fibre orientation angle it is not really a problem with shrinkage and stretch, you can work with that anyway since the effect on the angle is rather small.

Gary Baum PaperFuture Technologies (from the chair)

Can I comment on that? In the case of a machine-made paper, it is very simple to immerse it in water and then freely dry it so that you remove all the dried-in stresses, then you have a true fibre orientation. It has been done for 20–25 years. I think some of what you talked about we have been doing, but no one ever took the opportunity to actually measure fibre orientation and relate it to polar modulus.

Can you explain why those peanuts are leaning?

Torbjörn Wahlström

In this work, I only deal with the relation between the structure in the paper and its properties, I do not relate it to the process. However, in all these equations you can add $\gamma + \delta$ instead of γ and they can capture a leaning peanut.

Gary Baum

The lean angle just means you have a problem with your head-box.

Torbjörn Wahlström

In that you are right!

Gary Baum

I was hoping you would analyze those profiles you took in the z-direction. I thought you would explain why the fibre orientations are different as you go through the thickness direction in the sheet, but maybe that is the next paper.

Torbjörn Wahlström

What is so fascinating here is that despite the different fibre orientation in the thickness direction, still the mean of it seems to be very simple to predict based on the mean fibre orientation anisotropy.

Gary Baum

Is that in your next paper?

Torbjörn Wahlström

The pilot machine made paper in this study must have a profile in z-direction, still the mean distribution could be predicted based on MD and CD stiffness. Regarding the question about how the fibre orientation is created, that has not been dealt with in this work. I leave that to the research groups working with the relationship between process and fibre orientation, that is a much tougher task than this!